Reconstruction and alignment of vacancies in carbon nanotubes

Alex Taekyung Lee, Yong-Ju Kang, and K. J. Chang*
Department of Physics, Korea Advanced Institute of Science and Technology, Daejeon 305-701, Korea

In-Ho Lee
Division of Advanced Technology, Korea Research Institute of Standards and Science, Daejeon 305-600, Korea
(Received 27 November 2008; revised manuscript received 3 February 2009; published 6 May 2009)

Vacancies in carbon nanotubes usually aggregate into larger vacancies. Using first-principles and tight-binding calculations, we investigate the alignment of missing atoms and the movement of pentagon-heptagon defects that are formed by reconstructions in large vacancy clusters V_n ($n \leq 36$), where n is the number of missing atoms. In nanotubes with small diameters, missing atoms have a tendency to form a serial network rather than a large hole due to the existence of large curvatures. It is generally found that the parallel alignment of missing atoms along the tube axis is energetically more favorable than the spiral alignment. Thus, the removal of atoms leads to the longitudinal movement of a pentagon-heptagon defect on the tube wall, which is in good agreement with the kink motion observed during superplastic deformation of single-wall nanotubes. The preference of the longitudinal motion of the pentagon-heptagon defect is more prominent in armchair tubes compared with other chiral tubes.

DOI: 10.1103/PhysRevB.79.174105 PACS number(s): 61.46.Fg, 61.48.De, 71.20.Tx, 71.15.Nc

I. INTRODUCTION

Studying atomic vacancies in carbon systems such as nanotubes and graphene is of great importance as these defects critically affect the electrical, chemical, and mechanical properties of nanostructured carbon materials. Carbon vacancies are easily generated by ion or electron irradiation[1–5] and induce structural changes such as the shrinkage and bending of nanotubes and the compression of carbon onions.[6–9] The mechanical properties of nanotubes typically deteriorate as a result of vacancies, which particularly reduces the tensile strength.[10] On the other hand, electron irradiation gives rise to improvements in the mechanical properties of nanotube bundles and multiwall nanotubes by creating intertube links.[1,11,12]

When carbon vacancies are generated, nanotubes are self-healed via the reconstruction of the atomic network. This allows for the saturation of dangling bonds and the creation of topological defects, for example, a pentagon-heptagon defect. The existence of a topological defect has been observed directly by high-resolution transmission electron microscopy (HRTEM) at the junction of two nanotube segments with different diameters and chiralities.[2] Recent experiments reported that single-wall nanotubes that are tensile loaded at a high temperature undergo superplastic deformation and that kink motion is the universal plastic deformation mode, propagating in either a longitudinal direction or along a spiral path on the tube walls.[13–15]

In previous theoretical calculations, single vacancy, divacancy, and vacancy-interstitial defects were studied. Simple tight-binding (TB),[16] generalized gradient approximation within the density-functional theory (DFT) (Refs. 17–20) and density-functional-based tight-binding (DFTB) (Refs. 20 and 21) calculations showed that the formation energies of the single vacancy and divacancy defects depend on the tube diameter, on the chirality, and on the family. The formation energies in armchair tubes generally increase as the diameter increases, whereas they fluctuate in zigzag tubes. Recent DFTB calculations showed that a multivacancy formed by six missing atoms split into smaller defects of pentagon-heptagon defects.[21] A similar separation of a larger vacancy cluster formed by 12 missing atoms into two pentagon-heptagon defects was also found in tight-binding molecular dynamics simulations.[22,23] Although the longitudinal motion of the kinks observed in the superplastic deformation was considered to be related to the motion of the pentagon-heptagon defect due to the removal of atoms, the spiral motion of the kinks could not be explained in the molecular-dynamics simulations. The topological defect was also held to play a key role in the superplastic deformation of nanotubes; based on dislocation theory, the kink movement was described in terms of the glide of pentagon-heptagon defects and their pseudoclimb.[24,25] As superplastic deformation occurs at high temperatures, the lowest energy as well as metastable structures of vacancies may play a role in nucleating the kinks. Thus, it is important to conduct a comprehensive study of the alignment of missing atoms and its chirality dependence in vacancy clusters.

This study reports the results of first-principles and tight-binding calculations for the energetics, reconstruction, and orientation of vacancies formed by as many as 36 missing atoms in carbon nanotubes with different chiralities. Considering various atomic structures, it was found that missing atoms tend to be serially connected along the tube axis, regardless of the chirality. Comparing the lowest-energy structures, the formation of vacancy clusters in nanotubes with small diameters is proposed to take place via the diffusion and coalescence of single vacancies. Based on the results for the alignment of the missing atoms and the formation of reconstructed vacancy clusters, the preferential movement of pentagon-heptagon defects during the superplastic deformation of single-wall nanotubes is discussed.

II. CALCULATION METHOD

For small vacancy clusters V_n ($n \leq 6$), which are formed by removing n carbon atoms, first-principles calculations

 ©2009 The American Physical Society

within the density-functional-theory framework were made. The generalized gradient approximation (GGA) (Ref. 26) for the exchange-correlation potential and ultrasoft pseudopotentials was used,[27] as implemented in the VASP code.[28] The wave functions were expanded in plane waves up to an energy cutoff of 400 eV. Supercell geometries containing 8–11 unit cells for the (5,5) nanotube and 5–7 unit cells for the (9,0) nanotube were utilized. In tight-binding cluster calculations,[29] the numerical accuracy for small vacancy clusters was investigated. The vacancy size was then increased to $n=36$ for nanotubes with different chiralities. In this case, capped nanotubes were used in which two capped tube ends are fixed without relaxation in a manner similar to the periodic boundary conditions. When twisting or bending distortion is significant, capped nanotubes with the tube ends in a fully relaxed state were also tested. The ionic coordinates were optimized until the residual forces were less than 0.02 eV/Å. The stability of the vacancy clusters was examined by calculating the formation energy, which is defined as

$$E_f(V_n) = E_{\text{tot}}(V_n) - E^0_{\text{tot}} + n\mu_{\text{C}}, \tag{1}$$

where $E_{\text{tot}}(V_n)$ and E^0_{tot} refer to the total energies of the supercells with and without the defect V_n, respectively, and μ_{C} is the carbon chemical potential obtained from a pristine nanotube. For the capped end model, μ_{C} was determined by the following method. First we chose two capped tubes with the same caps but different tube lengths. As the strain effect near the cap region does not affect the middle segment of the tube, the energy difference between the two capped tubes can represent the carbon chemical potential.

III. RESULTS AND DISCUSSION

First, a single vacancy (V_1) is examined because it provides important information regarding the atomic structure of $V_n(n \geq 2)$. An ideal single vacancy is energetically unstable with respect to a reconstructed structure with a new bond formed by the elimination of two dangling bonds.[16–18,20,21] The orientation and bond length of the reconstructed bond (henceforth referred to as the rebond) strongly depend on the tube chirality and diameter. In nanotubes, the reconstructed bond can have three different orientations: parallel (∥), diagonal (//), and perpendicular (⊥) with respect to the tube axis. These are equivalent in graphene. As the orientation angle of the rebond with respect to the tube axis increases, its bond length generally decreases due to the curvature. In the (5,5) nanotube, the $V_1(5\text{-}9)^{//}$ defect [Fig. 1(a)], with a diagonal rebond of 1.55 Å, is more stable by 1.42 eV compared to the $V_1(5\text{-}9)^{\parallel}$ defect with a parallel rebond of 1.75 Å. In the (9,0) nanotube, the curvature effect on reconstruction is stronger than that of the armchair tube. The $V_1(5\text{-}9)^{\perp}$ defect [Fig. 2(a)] with a perpendicular rebond of 1.52 Å is lower in energy by 1.1 eV compared to the $V_1(5\text{-}9)^{//}$ defect with a diagonal rebond of 1.68 Å. Thus, the energy difference between different configurations is closely related to the difference in the rebond length. The effects of curvature and bond orientation on the stability of reconstructed bonds are similar to those found for functional groups such as CH_2 and NH, which, in armchair tubes, bind into an orthogonal C-C bond rather than a slanted C-C bond relative to the tube axis.[30,31]

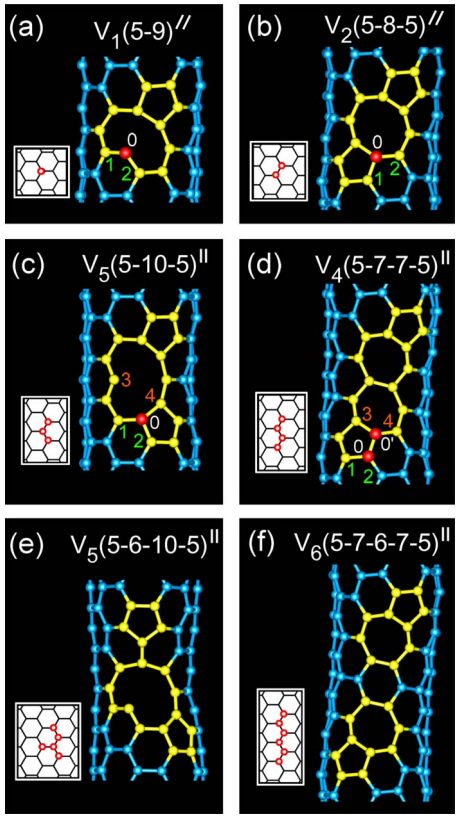

FIG. 1. (Color online) The lowest-energy structures of vacancies (V_n, $n=1-6$) in the (5,5) carbon nanotube. The missing atoms are serially connected along the tube axis, with the exception of V_5.

For $n \geq 2$, the defect orientation is defined as the angle (θ) of the longest chain of missing atoms relative to the tube axis. In this case, $\theta=0$ and 90° for parallel (∥) and perpendicular (⊥) alignments, respectively, and $0 < \theta < 90°$ for spiral (//) alignments. The most stable structures of V_n ($n \leq 6$) determined from the GGA calculations are compared for the (5,5) and (9,0) tubes in Figs. 1 and 2, respectively. In tubes with small diameters, a tendency was observed in which the missing atoms form a serial network along the tube axis rather than a large hole, which is more favorable in tubes with large diameters and in graphene. The V_n defect is easily obtained by removing the atom labeled 0 and forming a new bond between the atoms labeled 1 and 2 in the smaller V_{n-1} defect, with the exception of V_5 in the (5,5) tube, which will be discussed shortly. In case of V_4, an additional new bond is formed between the atoms labeled 3 and 4 in V_3. The stability of V_n tends to increase as the orientation angle θ increases, similar to V_1. Thus, the orientation and bond length of reconstructed bonds in pentagons play an important role in determining the alignment of missing atoms.

When n is even, it is clear that reconstruction completely eliminates the dangling bonds and leads to the formation of a pair of pentagon-heptagon defects, especially for $n=4$ and 6. In fact, the separation between the two pentagon-heptagon defects increases as n increases, which is in good agreement with previous calculations.[21–23] For a divacancy (V_2), two single vacancies coalesce into a 5-8-5 defect [$V_2(5\text{-}8\text{-}5)$],

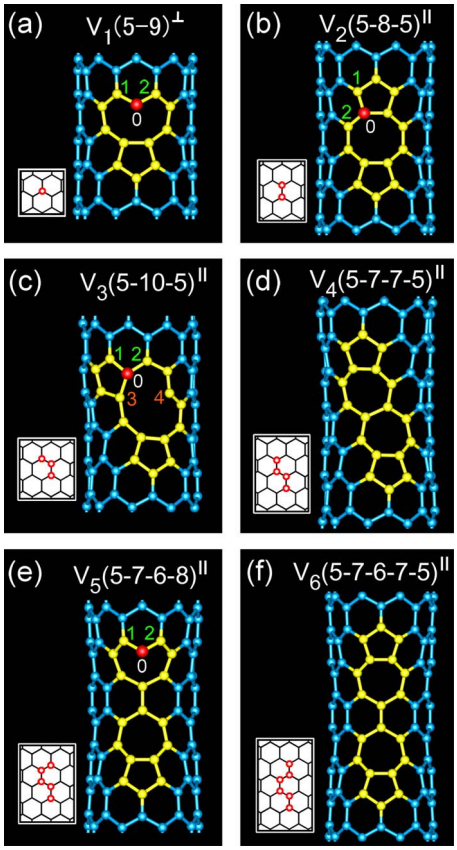

FIG. 2. (Color online) The lowest-energy structures of vacancies (V_n, $n=1-6$) in the (9,0) carbon nanotube. The missing atoms are serially connected along the tube axis.

which is composed of two pentagons and an octagon ring. In the (5,5) tube, the lowest-energy structure is the $V_2(5\text{-}8\text{-}5)^{//}$ defect with two diagonal rebonds of 1.51 Å. This defect is more stable by 2.45 eV compared to the $V_2(5\text{-}8\text{-}5)^{\perp}$ defect with two long parallel rebonds of 1.61 Å. Similarly, in the (9,0) tube, the $V_2(5\text{-}8\text{-}5)^{\parallel}$ defect with the perpendicular rebonds of 1.47 Å is more stable by 2.18 eV relative to the $V_2(5\text{-}8\text{-}5)^{//}$ defect. For a tetravacancy (V_4), the most stable $V_4(5\text{-}7\text{-}7\text{-}5)^{\parallel}$ defect consists of two pentagons and two heptagons that are serially connected along the axis. As the parallel alignment of the missing atoms induces local shrinkage in the nanotube, the rebonds are shortened considerably. The tube shrinkage is more significant in the (9,0) tube, which has perpendicular rebonds. In the $V_4(5\text{-}7\text{-}7\text{-}5)^{\perp}$ defect, as the missing atoms are connected along the circumference, the tube is bent by reconstruction. In case of a hexavacancy (V_6), the parallel alignment of the missing atoms along the tube axis is lower in energy compared to vacancy clusters in which the missing atoms are aggregated. The atoms surrounding the missing atoms reconstruct to heal the vacancy hole and eventually lead to a $V_6(5\text{-}7\text{-}6\text{-}7\text{-}5)^{\parallel}$ defect [Figs. 1(f) and 2(f)] in which two pentagon-heptagon defects are separated by a hexagon. In the (9,0) tube, as the alignment of the pentagon-heptagon defects is parallel to the tube axis, the rebonds are oriented along the circumference, with the small bond length of 1.446 Å. On the other hand, in the (5,5) tube, the orientation of each pentagon-heptagon defect is slightly tilted with respect to the axis, resulting in a larger rebond length of 1.477 Å. The $V_6(5\text{-}7\text{-}6\text{-}7\text{-}5)^{\parallel}$ defect was also found to be the most stable defect for tubes with large diameters, such as (10,10) and (16,0).[21–23]

When n is odd, one dangling bond remains at a large hole, as in a eight-, nine-, or ten-membered ring. A trivacancy defect [$V_3(5\text{-}10\text{-}5)$] consists of two pentagons and a ten-membered ring. Between two alignments of the missing atoms, $V_3(5\text{-}10\text{-}5)^{\parallel}$ and $V_3(5\text{-}10\text{-}5)^{\perp}$, the $V_3(5\text{-}10\text{-}5)^{\parallel}$ defect with a shorter rebond is more stable in the (5,5) and (9,0) nanotubes. The energy difference between $V_3(5\text{-}10\text{-}5)^{\parallel}$ and $V_3(5\text{-}10\text{-}5)^{\perp}$ is 1.21 eV in the (5,5) tube, as compared to the DFTB result of 1.93 eV.[21] Removal of an atom from $V_4(5\text{-}7\text{-}7\text{-}5)^{\parallel}$ along the axis leads to the $V_5(5\text{-}7\text{-}6\text{-}8)^{\parallel}$ defect, where an octagon ring is separated from a pentagon-heptagon defect [Fig. 2(e)]. In the (9,0) tube, the $V_5(5\text{-}7\text{-}6\text{-}8)^{\parallel}$ defect is lowest in energy due to the perpendicular rebond. In the (5,5) tube, however, the $V_5(5\text{-}7\text{-}6\text{-}8)^{\parallel}$ defect is less stable by 0.55 eV compared to the $V_5(5\text{-}6\text{-}10\text{-}5)^{\parallel}$ defect, as strains caused by twisting distortion in the $V_5(5\text{-}7\text{-}6\text{-}8)^{\parallel}$ defect are not properly released in finite-sized supercell calculations. From TB calculations for a larger supercell containing 55 unit cells, it was found that the energy difference is reduced to 0.22 eV. The $V_5(5\text{-}7\text{-}6\text{-}8)^{\parallel}$ defect with the parallel alignment of the missing atoms is also likely to be energetically favorable for a sufficiently long tube.

The formation energies of V_n are compared for the most stable structures in the (5,5) and (9,0) tubes in Fig. 3(a). The results of the TB calculations are similar to those obtained from the first-principles calculations. As n increases, the energies increase in an oscillatory manner because they are generally higher for odd numbers of n due to an unsaturated dangling bond. Although it requires additional energy to form a larger vacancy cluster, the formation energies per missing atom decrease as n increases, indicating that the formation of a larger vacancy cluster is energetically more favorable. Thus, in nanotubes under continuous electron irradiation, it is expected that vacancies will grow by capturing single vacancies, which are more mobile relative to divacancies.[20] In such a case, the missing atoms have a tendency to be serially connected along the tube axis, as shown in Figs. 1 and 2.

To observe the preference of the parallel alignment of the missing atoms to the spiral alignment, the TB calculations were extended to $n=36$, which results in numerical accuracy that is similar to that of the GGA calculations [Fig. 3(a)]. There are many ways to construct the vacancy structure for n as large as 36. However, it is difficult to test all possible configurations. If the missing atoms are not linearly connected, a lot of changes can be expected in the vacancy structure, such as the reorientation of reconstructed bonds, the generation of dangling bonds, and the deformation of nanotubes. These structural changes are likely to result in configurations which are less stable than the parallel and spiral alignments that were found for small vacancy clusters. Thus, for large vacancy clusters with $n>6$, we used the trend that, for small n up to 6, the missing atoms are aligned along a tube network, parallel or spiral to the tube axis. When n is odd, vacancies have a dangling bond. In the (5,5) tube, the

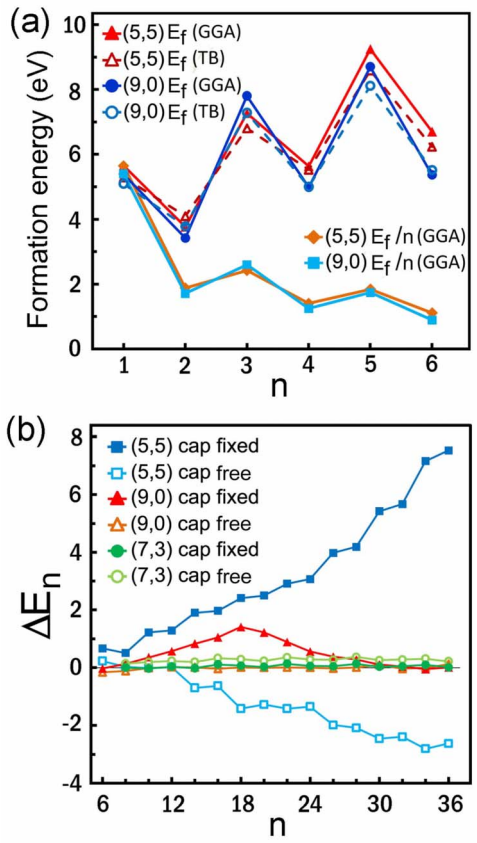

FIG. 3. (Color online) (a) The GGA formation energies (E_f) for the lowest-energy structures of V_n in the (5,5) and (9,0) nanotubes are compared with those obtained from the TB calculations. The formation energies per missing atom are denoted by E_f/n. (b) The TB results for the energy differences (ΔE_n) between the longitudinal and spiral alignments of the missing atoms are compared for the (5,5), (9,0), and (7,3) nanotubes; the filled (empty) points denote the results for the capped nanotubes in which the tube ends are fixed (fully relaxed).

existence of the dangling bond leads to the ground state different from the parallel alignment of the missing atoms, as shown for $n=5$ [Fig. 1(e)]. If n is large, the dangling bond would make it difficult to find the ground state due to more possible configurations. Thus, we considered the removal process of a pair of atoms, which eliminates the dangling bond, leading to the V_n ($n=$ even integer) defect.

In armchair tubes with a chiral angle of $\delta=30°$, the missing atoms form a serial network of the bond type $ABAB\cdots$ in the parallel alignment ($V_n^{\parallel}$), whereas the spiral alignment ($V_n^{//}$) at $\theta=30°$ consists of the missing bonds of the type $ABAC\cdots$ (Fig. 4). In chiral tubes including zigzag tubes, with chiral angles of $0\leq\delta<30°$, the parallel alignment requires a periodic mixture of the bond types A, B, and C, where the number (M) of the missing bonds of the types A and B equals an integer number close to $3/(\sqrt{3}\tan(30°-\delta))$ per bond of type C. In this case, the spiral alignment at $\theta=30°-\delta$ is precisely equivalent to the parallel alignment (of type $ABAB\cdots$) in the armchair tube. Depending on the alignment of the missing atoms, a pentagon-heptagon defect can move along either a longitudinal or a spiral path. In the (9,0) and

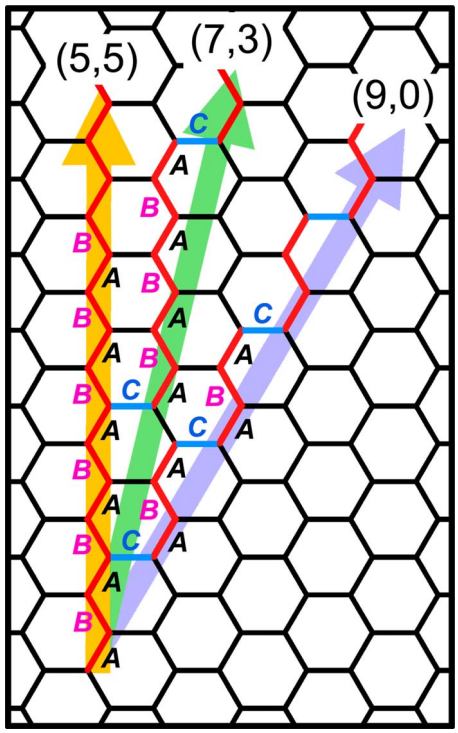

FIG. 4. (Color online) The arrows denote the tube axes of the (5,5), (7,3), and (9,0) nanotubes, the chiral angles of which are defined as relative angles of the tube axes with respect to the zigzag tube. The longitudinal and spiral alignments of missing atoms are represented by a combination of the missing bonds labeled as A, B, and C around each atomic site.

(5,5) tubes, the periods of the spiral movement are $n=34$ and 36, respectively. Thus, two pentagon-heptagon defects are located on the opposite sides of the tube wall when $n=16$ and 18 in the (9,0) tube [Fig. 5(a)] and when $n=18$ in the (5,5) tube [Fig. 6(a)].

Regardless of the tube chirality, it was found that the parallel alignment of the missing atoms is energetically more favorable than the spiral alignment [Fig. 3(b)]. However, the energy differences (ΔE_n) between the $V_n^{\parallel}$ and $V_n^{//}$ defects are sensitive to the type of tube. There are two major contributions to ΔE_n that are related to the reconstructed bond formed by the removal of the bond type C and by the twisting distortion induced by the spiral alignment. If the bond length of the reconstructed bond increases due to a change in the orientation, the defect stability is reduced. Essentially, the contribution of the reconstructed bond to ΔE_n decreases as δ decreases, resulting in no effect on the zigzag tubes with $\delta=0$. If the $V_n^{\parallel}$ defect contains missing bonds of type C, twisting distortion is generally suppressed, stabilizing the parallel alignment. In armchair tubes, however, twisting distortion is enhanced because the missing bonds of type C appear in the spiral alignment.

In the (9,0) tube, ΔE_n gradually increases to $n=18$ and then decreases to zero when $n=34$ and 36, exhibiting oscillatory behavior when $n>36$. As mentioned earlier, there is no difference in the bond length of the reconstructed bonds between the $V_n^{\parallel}$ and $V_n^{//}$ defects, even in the presence of missing bonds of type C in the $V_n^{\parallel}$ defect. As the intermediate

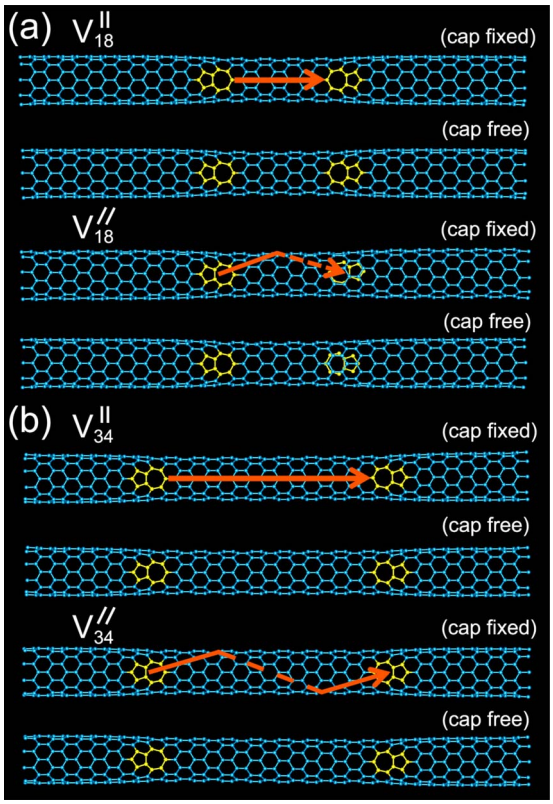

FIG. 5. (Color online) (a) and (b) The atomic structures of the $V_n^{\parallel}$ and $V_n^{//}$ defects are compared for $n=18$ and 34 in the (9,0) nanotube. In the TB calculations, two different boundary conditions are used for a capped nanotube in which the tube ends are fixed or fully relaxed. The arrows denote the longitudinal and spiral paths of the pentagon-heptagon defect, as induced by subsequent removal of a pair of atoms in the $V_n^{\parallel}$ and $V_n^{//}$ defects, respectively.

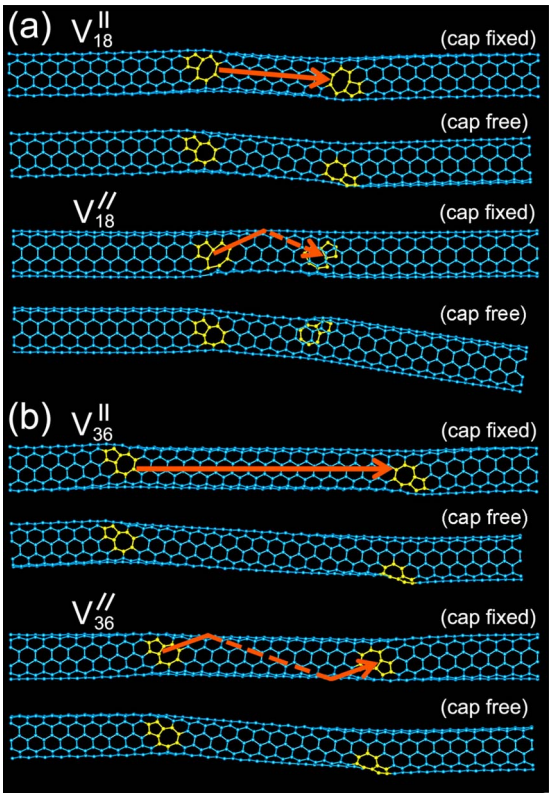

FIG. 6. (Color online) (a) and (b) The atomic structures of the $V_n^{\parallel}$ and $V_n^{//}$ defects are compared for $n=18$ and 36 in the (5,5) nanotube. In the TB calculations, two different boundary conditions are used for a capped nanotube in which the tube ends are fixed or fully relaxed. The arrows denote the longitudinal and spiral paths of the pentagon-heptagon defect, as induced by subsequent removal of a pair of atoms in the $V_n^{\parallel}$ and $V_n^{//}$ defects, respectively.

tubes precisely correspond to the (8,0) tube, with the same tube lengths and diameters, the $V_n^{\parallel}$ and $V_n^{//}(\theta=30°)$ defects are identical when $n=34$ and 36 [Fig. 5(b)]. The major contribution to ΔE_n is the twisting distortion in the spiral alignment. However, as the induced twisting distortion is weak due to the absence of bond type C, the energy differences are relatively small, within 1.41 eV between the $V_n^{\parallel}$ and $V_n^{//}$ defects. On the other hand, in the (5,5) tube, the intermediate tubes in the $V_{36}^{\parallel}$ and $V_{36}^{//}$ defects are not equivalent to each other due to different twisting distortions, although their chiralities are close to (5,4) [Fig. 6(b)]. In the $V_n^{//}$ defect, the intermediate tube shows more shrinkage and is shortened. Moreover, strains by twisting distortion accumulate whenever a type C bond is removed. Thus, ΔE_n continuously increases as n increases; reaching a value of 2.41 and 7.53 eV when $n=18$ and 36, respectively. In the (7,3) tube with a diameter similar to those of the (9,0) and (5,5) tubes, the parallel network of the missing atoms is expected to be of the type $ABABABAC$ with $M=7$ (Fig. 4). In the $V_n^{\parallel}$ defect, removal of type C bond weakens the reconstructed bond. However, such an effect is less significant than that of the (5,5) tube. Additionally, the twisting distortion caused by the alignment of type $ABABABA$ is weakened by the presence of the missing bond of type C. In the $V_n^{//}$ defect, the strain effect is also small due to the small spiral angle of $\theta=13°$, although there is no strain release. Thus, the variation in ΔE_n to within 0.15 eV is much smaller than those of the (9,0) and (5,5) tubes [Fig. 3(b)].

It should be noted that if tubes are sufficiently long, strains induced by twisting or bending distortion can be properly released; especially in the (5,5) tube, ΔE_n for $n=36$ is reduced from 7.53 to 5.21 eV and finally to 3.74 eV when the tube length increases from 8.1 to 10.8 nm and then to 13.5 nm, respectively. To accommodate twisting and bending distortions, the TB calculations were performed for the nanotubes, where the tube ends are in a fully relaxed state, similar to that of infinitely long tubes. In the (9,0) tube, as distortions are much smaller (Fig. 5), ΔE_n lies in the range between −0.16 and 0.12 eV, indicating that both the $V_n^{\parallel}$ and $V_n^{//}$ defects are energetically favorable. In the (7,3) tube, the $V_n^{\parallel}$ defect is more stabilized against the $V_n^{//}$ defect, increasing the variation range of ΔE_n to 0.37 eV. On the other hand, in the (5,5) tube, the tube is well twisted and bent in the spiral configuration (Fig. 6). Thus, the stability of the $V_n^{//}$ defect is greatly enhanced, with ΔE_n decreasing to −2.7 eV when $n=36$.

It was reported that superplastic deformation of nanotubes is promoted by both thermal energy and tensile strain.[13,14] We tested the effect of tensile strain on the energetics of the parallel and spiral alignments of the missing atoms. If strain

is applied to the (5,5) tube, the bond lengths of the rebonds in the parallel alignment increase more than those in the spiral alignment. For a strain of 5%, ΔE_n is enhanced by 1.80, 1.81, and 3.39 eV for $n=6$, 8, and 10, respectively, keeping the same tendency as that found for the unstrained case. In the (9,0) tube, as the orientation angles of the reconstructed bonds are the same in the parallel and spiral alignments, ΔE_n is not much affected by strain. Thus, our results indicate that, under tensile strain, the missing atoms still prefer the parallel alignment to the spiral one. Here we point out that large-scale molecular mechanics simulations using empirical potentials such as the Tersoff-Brenner potential may be useful to investigate the effect of tensile strain on ΔE_n for large vacancy clusters. In nanotubes which are tensile loaded, molecular mechanics simulations[32] showed that the formation of a Stone-Wales defect becomes energetically favored as strain increases, in good agreement with the results predicted by first-principles and tight-binding calculations.

As the separation between two pentagon-heptagon defects increases with n, nanotubes continue to shrink in the intermediate region. In recent HRTEM experiments, a pentagon-heptagon defect was observed at the junction of the (17,0) and (18,0) nanotubes that was produced by electron irradiation.[2] In zigzag tubes, it is difficult to distinguish the parallel and spiral alignments of the missing atoms by observing only a pentagon-heptagon defect at one junction, as these alignments lead to similar pentagon-heptagon defects at the junction. As the $V_n^{\parallel}$ defect is lower in energy relative to the $V_n^{//}$ defect, the pentagon-heptagon defect observed at room temperature is likely to be related to the parallel alignment of the missing atoms. In nanotubes with very large diameters, the serial alignment of the missing atoms will be suppressed as the curvature effect is weakened. In fact, very recent experiments demonstrated the migration and coalescence of large holes on the outer tube wall of double-wall nanotubes with diameters close to 70 Å.[33]

When single-wall nanotubes undergo superplastic deformation, both the longitudinal and spiral motions of kinks along the tube wall were observed.[13,14] If the kinks are related to pentagon-heptagon defects, the motion of kinks can be explained by the present results concerning the alignment of the missing atoms. Due to the preference of the parallel alignment of the missing atoms, the pentagon-heptagon defect is more likely to propagate along a longitudinal path on the tube wall (Figs. 5 and 6), accompanied with the tube shrinkage induced by the removal of atoms. The preference of the longitudinal motion of the pentagon-heptagon defect is more prominent in armchair tubes. This kink motion is actually equivalent to the climb motion of the pentagon-heptagon defect, which is induced by subsequently evaporating a C_2 dimer.[24,25]

It was shown that the pentagon-heptagon defect glides along the dislocation line, perpendicular to the orientation of the pentagon-heptagon defect, by Stone-Wales bond rotations that preserve the total mass but induce shrinkage and stepwise necking of the tube.[24,34,35] The glide motion alone has difficulty explaining the longitudinal motion of kinks, which is accompanied with the tube elongation. This difficulty is attributed to the fact that, in general, the Burgers vectors are not parallel to the tube axis. In armchair tubes, there is one Burgers vector parallel to the tube axis. If the glide motion takes place along this Burgers vector, it is possible for the pentagon-heptagon pair of the Stone-Wales defect to move along the tube axis. However, kinks cannot be produced and only bending distortion is induced, without reducing the tube diameter. On the other hand, in other chiral tubes, there exists no Burgers vector parallel to the tube axis, resulting in the spiral movement of kinks. In zigzag tubes, while the gliding direction of the Stone-Wales defect is 30° off the tube axis, the pentagon-heptagon defects in the vacancy cluster V_n glide along the circumference, as shown in V_4 and V_6 [Figs. 2(b) and 2(d)]. Previous studies addressed the limitation of the glide motion in explaining the longitudinal movement of kinks.[14,24] To describe the longitudinal kink motion, Huang *et al.*[14] suggested the aggregation of vacancies, similar to the alignment of the missing atoms in our work. In other study, Ding *et al.*[24] showed that both the glide and climb motions can generate kinks and reduce the tube diameter, inducing the longitudinal movement of kinks

When the glide motion is combined with the removal of atoms, the missing atoms can form a spiral network. In this case, the spiral kink motion is also considered as a result of the spiral alignment of the missing atoms, where C_2 dimers are continuously removed along the spiral direction. In zigzag tubes, the possibility of the spiral movement of the pentagon-heptagon defect is enhanced at high temperatures due to the small energy differences between the $V_n^{\parallel}$ and $V_n^{//}$ defects. In chiral tubes with small chiral angles, both the longitudinal and spiral kink motions are also likely to appear as only a small amount of energy is required for a pentagon-heptagon defect to glide. However, when the spiral angle is very small, it is difficult to distinguish between the $V_n^{//}$ and $V_n^{\parallel}$ defects. On the other hand, in armchair tubes, the spiral movement of the pentagon-heptagon defect will be suppressed due to accumulated strains unless the tube is sufficiently long to accommodate bending and twisting distortions.

IV. CONCLUSIONS

In conclusion, the atomic structure of large vacancy clusters and the preference of various alignments of the missing atoms in carbon nanotubes with small diameters were studied using the generalized gradient approximation and tight-binding calculations. It was found that vacancies tend to aggregate to form vacancy clusters, where the missing atoms are aligned along the tube axis. The stability of vacancies is strongly affected by the existence of dangling bonds, the orientation of the missing atoms, and the alignment of the reconstructed bonds in pentagons. Based on the results for the vacancy structures, it is suggested that in small-diameter nanotubes, vacancy clusters grow via the diffusion and coalescence of single vacancies. When tubes shrink as a result of the removal of atoms along the tube, it was found that a pentagon-heptagon defect that forms at the junction of two nanotube segments with different diameters and chiralities can propagate either along a longitudinal path or along a

spiral path. Calculations further showed that the longitudinal motion of the pentagon-heptagon defect is energetically more favorable than the spiral motion, in good agreement with experiments.

ACKNOWLEDGMENTS

This work was supported by the Korea Research Foundation (Grant No. KRF-2005-084-C00007).

*kchang@kaist.ac.kr

[1] A. V. Krasheninnikov and F. Banhart, Nature Mater. **6**, 723 (2007).
[2] A. Hashimoto, K. Suenaga, A. Gloter, K. Urita, and S. Iijima, Nature (London) **430**, 870 (2004).
[3] K. Suenaga, H. Wakabayashi, M. Koshino, Y. Sato, K. Urita, and S. Iijima, Nat. Nanotechnol. **2**, 358 (2007).
[4] M. Terrones, H. Terrones, F. Banhart, J.-C. Charlier, and P. M. Ajayan, Science **288**, 1226 (2000).
[5] L. Sun, F. Banhart, A. V. Krasheninnikov, J. A. Rodríguez-Manzo, M. Terrones, and P. M. Ajayan, Science **312**, 1199 (2006).
[6] P. M. Ajayan, V. Ravikumar, and J.-C. Charlier, Phys. Rev. Lett. **81**, 1437 (1998).
[7] F. Banhart, J. X. Li, and A. V. Krasheninnikov, Phys. Rev. B **71**, 241408(R) (2005).
[8] J. Li and F. Banhart, Nano Lett. **4**, 1143 (2004).
[9] T. D. Yuzvinsky, W. Michelson, S. Aloni, G. E. Begtrup, A. Kis, and A. Zettl, Nano Lett. **6**, 2718 (2006).
[10] M. Sammalkorpi, A. Krasheninnikov, A. Kuronen, K. Nordlund, and K. Kaski, Phys. Rev. B **70**, 245416 (2004).
[11] K. Urita, K. Suenaga, T. Sugai, H. Shinohara, and S. Iijima, Phys. Rev. Lett. **94**, 155502 (2005).
[12] M. Huhtala, A. V. Krasheninnikov, J. Aittoniemi, S. J. Stuart, K. Nordlund, and K. Kaski, Phys. Rev. B **70**, 045404 (2004).
[13] J. Y. Huang, S. Chen, Z. Q. Wang, K. Kempa, Y. M. Wang, S. H. Jo, G. Chen, M. S. Dresselhaus, and Z. F. Ren, Nature (London) **439**, 281 (2006).
[14] J. Y. Huang, S. Chen, Z. F. Ren, Z. Q. Wang, D. Z. Wang, M. Vaziri, Z. Suo, G. Chen, and M. S. Dresselhaus, Phys. Rev. Lett. **97**, 075501 (2006).
[15] J. Y. Huang, S. Chen, Z. F. Ren, Z. Wang, K. Kempa, M. J. Naughton, G. Chen, and M. S. Dresselhaus, Phys. Rev. Lett. **98**, 185501 (2007).
[16] A. J. Lu and B. C. Pan, Phys. Rev. Lett. **92**, 105504 (2004).
[17] Y. Ma, P. O. Lehtinen, A. S. Foster, and R. M. Nieminen, New J. Phys. **6**, 68 (2004).
[18] J. M. Carlsson, Phys. Status Solidi B **243**, 3452 (2006).
[19] R. G. Amorim, A. Fazzio, A. Antonelli, F. D. Novaes, and A. J. R. da Silva, Nano Lett. **7**, 2459 (2007).
[20] A. V. Krasheninnikov, P. O. Lehtinen, A. S. Foster, and R. M. Nieminen, Chem. Phys. Lett. **418**, 132 (2006).
[21] J. Kotakoski, A. V. Krasheninnikov, and K. Nordlund, Phys. Rev. B **74**, 245420 (2006).
[22] G.-D. Lee, C.-Z. Wang, J. Yu, E. Yoon, N.-M. Hwang, and K.-M. Ho, Phys. Rev. B **76**, 165413 (2007).
[23] G.-D. Lee, C. Z. Wang, E. Yoon, N.-M. Hwang, and K. M. Ho, Appl. Phys. Lett. **92**, 043104 (2008).
[24] F. Ding, K. Jiao, M. Wu, and B. I. Yakobson, Phys. Rev. Lett. **98**, 075503 (2007).
[25] F. Ding, K. Jiao, Y. Lin, and B. I. Yakobson, Nano Lett. **7**, 681 (2007).
[26] J. P. Perdew, K. Burke, and M. Ernzerhof, Phys. Rev. Lett. **77**, 3865 (1996).
[27] D. Vanderbilt, Phys. Rev. B **41**, 7892 (1990).
[28] G. Kresse and J. Furthmüller, Phys. Rev. B **54**, 11169 (1996).
[29] C. Tang, W. Guo, and C. Chen, Phys. Rev. Lett. **100**, 175501 (2008).
[30] Y.-S. Lee and N. Marzari, Phys. Rev. Lett. **97**, 116801 (2006).
[31] T. Yumura and M. Kertesz, Chem. Mater. **19**, 1028 (2007).
[32] M. B. Nardelli, B. I. Yakobson, and J. Bernholc, Phys. Rev. Lett. **81**, 4656 (1998).
[33] C. Jin, K. Suenaga, and S. Iijima, Nano Lett. **8**, 1127 (2008).
[34] B. I. Yakobson, Appl. Phys. Lett. **72**, 918 (1998).
[35] S. Zhang and T. Zhu, Philos. Mag. Lett. **87**, 567 (2007).